

Three-Dimensional Broadband Solar Radiative Transfer in Small Tropical Cumulus Fields Derived From High-Resolution Imagery

*K. F. Evans and T. C. Benner
University of Colorado
Boulder, Colorado*

Introduction

Many previous radiative transfer studies (e.g., Welch and Wielicki 1984) have shown the potential for a significant error in plane-parallel modeling of solar fluxes from cloud fields. More recently, the independent pixel approximation (IPA; Cahalan et al. 1994) has been shown to be accurate for calculating domain average solar fluxes and heating rates in stratiform clouds. Attention is now turning toward deeper cumuloform cloud types, where the IPA might be expected to perform poorly, due to photon leakage from cloud sides and other three-dimensional (3-D) effects. The IPA has been shown to be surprisingly accurate in comparison with 3-D broadband solar calculations for a shallow cumulus and a deep convective cloud field (Barker et al. 1998). Thus, for different case studies the IPA has been shown to be adequate or gross in error, depending on the particular cloud type. The true magnitude of 3-D solar radiative transfer effects for actual cloud fields remains to be discovered.

Here we seek to determine the magnitude of the 3-D effect and the adequacy of various approximations for a statistically representative sample of a particular cloud type. The cloud fields studied are central tropical Pacific cumulus below the freezing level without overlying ice clouds.

Remote Sensing Cloud Structure

Realistic cloud structure was derived from Moderate-Resolution Imaging Spectroradiometer (MODIS) Airborne Simulator (MAS; King et al. 1996) imagery observed during Central Equatorial Pacific Experiment (CEPEX) from the ER-2 at 20-km altitude. The MAS data are high resolution (50 m at nadir), calibrated to high radiometric accuracy, and have high precision (10 bit) for the infrared channels. Visible (0.66 μm) and thermal infrared (11.0 μm) channels were used to retrieve liquid water path (LWP) and cloud thickness. For each flight segment, plane-parallel radiative transfer modeling was used to construct a look up table relating the MAS radiances to LWP and cloud thickness. The modeling included molecular absorption based on a mean Tropical Ocean Global Atmosphere-Coupled Ocean Atmosphere Response Experiment (TOGA-COARE) sounding for shallow cloud conditions. Molecular scattering was included, but aerosol scattering was not. Instead, the modeled ocean albedo and sea surface temperatures were adjusted to agree with the mean clear-sky radiances for each flight segment. The cloud LWP, based on a scaling of the adiabatic liquid water content (LWC) profile for

50 droplets/cm³, and cloud thickness were retrieved by matching look-up table radiances. The uniform cloud base of ≈ 700 m was determined from the sounding. The optical depth cutoff was 128, but otherwise superadiabatic clouds were allowed.

Thus 3-D cloud structure, albeit internally smooth, is obtained. We believe that the 3-D radiative transfer effects in cumulus depend mostly on the optical depth and boundary geometry of the clouds. Internal variability (inside more than one scaled mean free path) is probably not important due to diffusion. Of course, the cloud retrievals themselves are affected by 3-D radiative transfer effects such as radiative smoothing and cloud shadowing. The solar zenith angle is restricted to mostly less than 52° to reduce retrieval errors. Retrievals are made for 125 scenes of 500 x 500 pixels (in the center of the MAS scan) in 9 flight segments on March 11, 1993, and April 3, 1993. Table 1 lists statistics for cloud properties obtained from individual scenes. These scenes represent all of the data from the two flights without overlying cirrus and having solar zenith angles less than 60°. The statistics, however, may be biased toward convectively active regions, as those were the primary targets of CEPEX.

Property	Mean	Min.	Max.
Cloud fraction	0.110	0.003	0.397
Mean LWP (g/m ²)	2.91	0.027	15.8
Maximum LWP (g/m ²)	678	32	4200
Mean cloud optical depth	4.40	2.0	17.8
Standard deviation $\ln \tau_c$	0.64	0.29	1.25
Max cloud depth (km)	1.51	0.90	3.40

Solar Radiative Transfer

Broadband solar radiative transfer was calculated for the cloud fields derived from the MAS scenes. The 3-D cloud droplet distribution was derived from the LWP and cloud thickness fields by scaling an adiabatic LWC profile and using a gamma size distribution with 50 droplets/cm³. The broadband calculation was performed using Fu's correlated k-distribution (Fu and Liou 1992). Only 4 bands from 0.2 to 2.5 μm were used, since there is very little reflected flux in bands 5 and 6. The cloud droplet optical properties, including the full phase function, were calculated with Mie theory. Top of atmosphere reflected and total column absorbed solar fluxes were calculated with the maximal cross section Monte Carlo method. The Monte Carlo code calculates domain average fluxes for full 3-D radiative transfer, the IPA, the tilted independent pixel approximation (TIPA) (Varnai and Davies 1999), and plane-parallel with cloud fraction approximation. Fluxes were calculated for 5 solar zenith angles (0°, 27°, 45°, 56°, 63°) and a daytime average (overhead sun at noon). A 5% Lambertian surface albedo was assumed for all wavelengths. For each broadband flux calculation, 10⁶ photons were simulated, for a total of 10⁶ photons x 125 scenes x 6 solar angles x 4 radiative approximations = 3 x 10⁹ photons.

Results

The radiative transfer results averaged over all 125 scenes are shown in Figure 1 as a function of solar zenith angle. As expected, for overhead sun the plane-parallel reflected flux is greater than the IPA flux, which is greater than the 3-D flux. For overhead sun, the IPA error ignores 3-D-photon leakage out the cloud sides, while the plane-parallel error also includes the nonlinear optical depth-albedo relation effect. For larger solar zenith angles, the IPA error is negative because IPA ignores the higher effective cloud fraction intercepted by the sunlight. The TIPA operates on the optical path distribution at the solar zenith angle, and hence incorporates the higher effective cloud fraction for oblique sun angles. The TIPA albedo stays greater than the 3-D albedo due to its neglect of leakage out cloud sides.

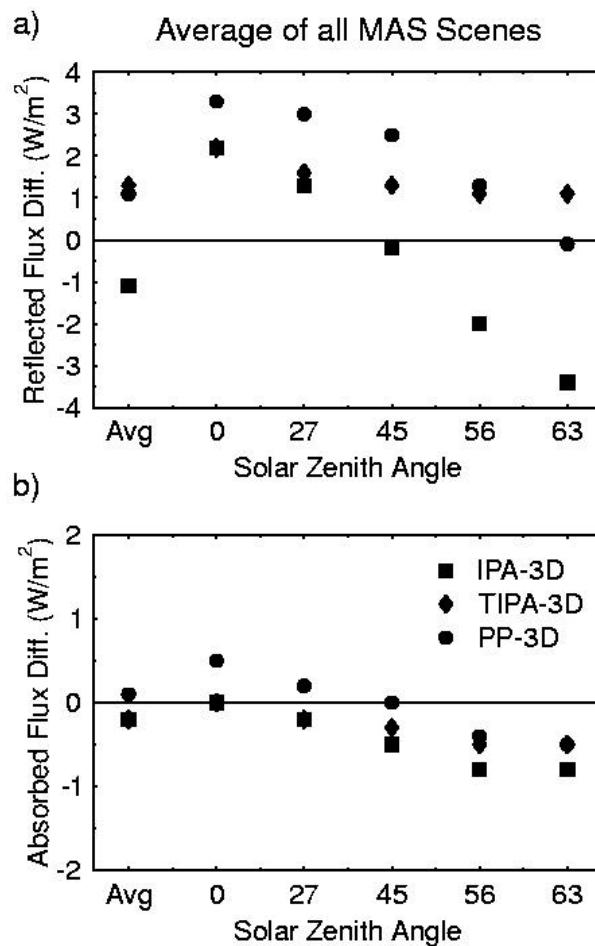


Figure 1. a) The difference between the 3-D reflected solar flux and various radiative transfer approximations for the average of all 125 MAS scenes. b) The difference between the 3-D column absorbed solar flux and various radiative transfer approximations for the average of all 125 MAS scenes. The results for the daytime average (Avg.) and 5 solar zenith angles are shown. PP = plane-parallel.

The most significant result is that all of the approximations (even plane-parallel [pp]) are within about 1 W/m^2 for the daytime average reflected flux. The 3-D radiative effects on the column absorption are even smaller. Fundamentally, the small 3-D effect is due to the low cloud fraction (averaging 11%), resulting in a mean scene daytime average reflected flux of 102 W/m^2 , compared to 87 W/m^2 for clear sky. The 3-D radiative transfer effect is also reduced by the distribution of cumulus cloud geometric depths tending towards thin clouds, which have less side leakage.

The individual scene reflected fluxes are shown in Figure 2. The daytime average plane-parallel flux errors may be as much as 10 W/m^2 higher than the 3-D fluxes for more reflective scenes. These scenes have higher cloud fraction, higher cloud optical depths, and deeper clouds. For the daytime average the TIPA overestimates albedo slightly, while the IPA underestimates slightly (the side leakage and effective cloud fraction effects partly cancel).

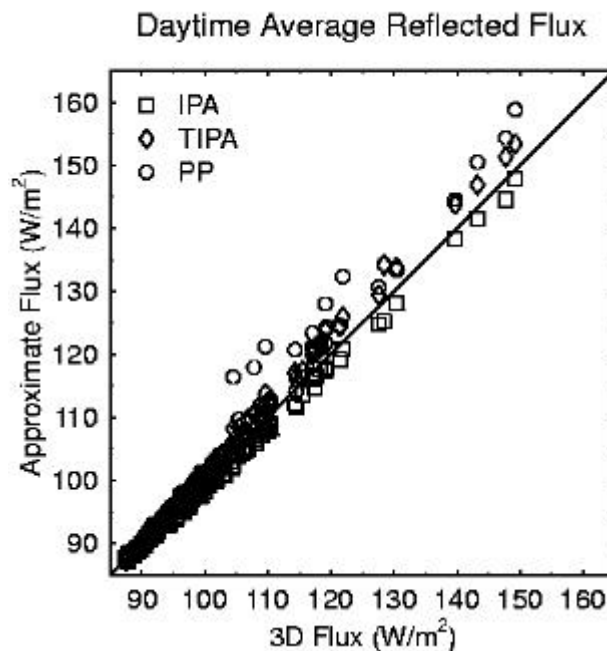


Figure 2. A scatter plot of IPA, TIPA, and PP broadband reflected flux vs. 3-D reflected flux for all 125 MAS scenes. PP = plane-parallel.

Given that some scenes have significant reflected flux errors when the IPA or TIPA are used, it would be desirable to correct these errors by relating them to some observable cloud field parameter. Figure 3 illustrates an empirical approach, for example, relating the IPA/TIPA flux errors to cloud fraction. In order to define the “radiatively significant” cloudy parts of the scenes, we apply a somewhat arbitrary optical depth threshold of 5 (which gives a scene cloud fraction mean of 0.029 and maximum of 0.167). The relationship between the IPA and TIPA flux errors and several parameters generated from the cloud scenes is investigated. Tables 2 to 4 list the correlation coefficient and the root mean square (rms) flux error for linear regressions with these parameters. Some of these cloud parameters are described in

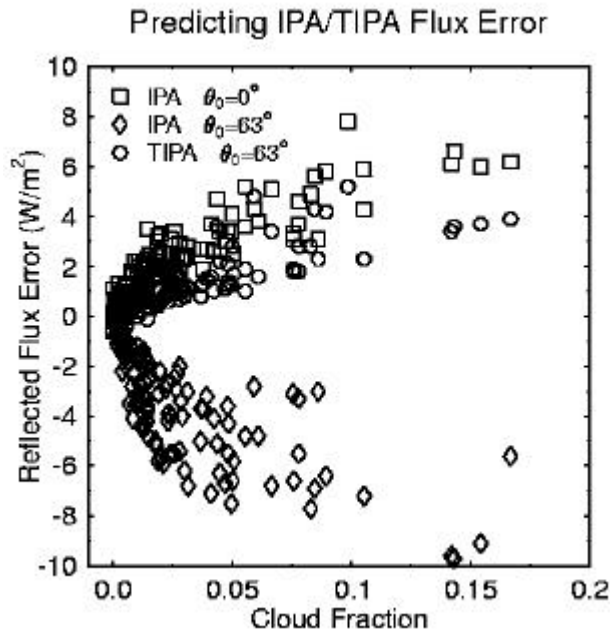


Figure 3. A scatter plot of IPA and TIPA broadband reflected flux error relative to 3-D as a function of cloud fraction for two solar zenith angles (TIPA is equivalent to IPA for overhead sun).

Table 2. Correlation and root mean square (rms) error results for solar zenith angle (SZA)= 0° IPA reflected flux error (IPA-3-D) regressions. Parameters are for the $\tau > 5$ threshold.

Cloud Parameter	Corr.	rms
Cloud fraction	0.875	0.81
Mean cloud τ	0.483	1.46
Fraction X mean τ	0.864	0.84
Cloud perimeter	0.839	0.90
Fractal dimension	0.065	1.66
Mean cloud depth	0.434	1.50
Area avg. max depth	0.632	1.29
Cloud side area	0.924	0.64
Upwelling flux	0.887	0.77

Table 3. Correlation and rms error results for SZA = 63° IPA and TIPA flux error regressions.

Cloud Parameter	IPA		TIPA	
	Corr.	rms	Corr.	rms
Cloud fraction	-0.754	1.68	0.853	0.57
Mean cloud τ	-0.285	2.45	0.695	0.78
Fraction X (τ)	-0.676	1.88	0.952	0.33
Cloud perimeter	-0.766	1.64	0.734	0.74
Fractal dimension	-0.121	2.53	0.067	1.09
Mean cloud depth	-0.497	2.21	0.395	1.00
Avg. max depth	-0.579	2.08	0.690	0.79
Cloud side area	-0.927	0.96	0.783	0.68
Upwelling flux	-0.879	1.22	0.790	0.67

Table 4. Correlation and rms error results for IPA/TIPA reflected flux error regressions over all five solar angles.

Cloud Parameter	IPA		TIPA	
	Corr.	rms	Corr.	rms
Cloud fraction	-0.049	2.67	0.815	0.80
Mean cloud τ	-0.022	2.67	0.560	1.14
Fraction X (τ)	-0.042	2.67	0.857	0.71
Cloud perimeter	-0.037	2.67	0.759	0.89
Fractal dimension	-0.017	2.67	0.078	1.37
Mean cloud depth	-0.132	2.65	0.363	1.28
Avg. max depth	-0.103	2.66	0.611	1.09
Cloud side area	-0.123	2.65	0.803	0.82
Upwelling flux	0.448	2.39	0.773	0.87

Benner and Curry (1998). The best predictors of IPA and TIPA reflected flux errors are cloud fraction, cloud fraction times mean cloud optical depth, upwelling flux, and cloud side area. The cloud side area is defined as the sum of the mean depth of each cloud times its perimeter. For oblique sun angles the TIPA rms errors are substantially lower than the IPA rms flux errors. Furthermore, if the regressions are performed for all five sun angles simultaneously, the TIPA errors are still well predicted, whereas those of IPA are not. Over the five sun angles the TIPA rms may be reduced to about 0.8 W/m² using regression against one of several cloud parameter, including cloud fraction and cloud fraction times mean optical depth. For comparison, over all scenes and the five sun angles, the TIPA bias error is 1.4 W/m² and the rms error is 2.0 W/m². Of course, regression relations based on these particular 125 MAS scenes are not necessarily generalizable to other cumulus cloud fields. On the other hand, the optical depth threshold and the selection of parameters have not been optimized to increase the predictability of the TIPA flux error.

Summary and Future Work

Broadband solar radiative transfer has been simulated in 125 scenes of tropical small cumulus clouds derived from 50-m resolution MAS imagery. Our focus was on the accuracy of plane-parallel, IPA, and TIPA as compared to 3-D radiative transfer. The daytime averaged reflected flux errors of all the approximations were only about 1 W/m^2 due to the low cloud fraction of the scenes. The plane-parallel radiative transfer error in column absorption is negligible. The TIPA reflected flux was found to be consistently slightly larger than the 3-D flux, whereas the IPA flux error changes sign with sun angle. Thus, TIPA appears to be a useful basis for a parameterization of 3-D radiative transfer effects. Regressions based on reflected flux, cloud fraction, and cloud side areas were found to be good predictors of the TIPA error. In the future, it would be useful to quantify errors from the plane-parallel cloud retrieval methodology and the effect of ignoring internal cloud variability. More generally, we believe this type of assessment of 3-D radiative effects for statistically complete cloud types should be pursued to determine the true magnitude of the 3-D radiation-cloud problem.

Acknowledgments

This work was supported by a National Science Foundation (NSF) grant ATM-9421733, a U.S. Department of Energy (DOE) Atmospheric Radiation Measurement (ARM) grant (KFE), and a National Aeronautics and Space Administration (NASA) Earth System Science Fellowship (TCB).

References

- Barker, H. W., J. J. Morcrette, and G. D. Alexander, 1998: Broadband solar fluxes and heating rates for atmospheres with 3-D broken clouds. *Q. J. R. Meteorol. Soc.*, **124**, 1245-1271.
- Benner, T. C., and J. A. Curry, 1998: Characteristics of small tropical cumulus clouds and their impact on the environment. *J. Geophys. Res.*, **103**, 28,753-28,767.
- Cahalan, R. F., W. Ridgeway, W. J. Wiscombe, T. L. Bell, and J. B. Snider, 1994: The albedo of fractal stratocumulus clouds. *J. Atmos. Sci.*, **51**, 2434-2455.
- Fu, Q., and K. N. Liou, 1992: On the correlated k-distribution method for radiative transfer in nonhomogeneous atmospheres. *J. Atmos. Sci.*, **49**, 2139-2156.
- King, M. D. et al., 1996: Airborne scanning spectrometer for remote sensing of cloud, aerosol, water vapor, and surface properties. *J. Atmos. Ocean Tech.*, **13**, 777-793.
- Varnai, T., and R. Davies, 1999: Effects of cloud heterogeneities on shortwave radiation: Comparison of cloud top variability and internal heterogeneity. *J. Atmos. Sci.* In press.
- Welch, R. M., and B. A. Wielicki, 1984: Stratocumulus cloud field reflected fluxes: The effect of cloud shape. *J. Atmos. Sci.*, **21**, 3086-3103.